An Unstable Anion Stabilized in a Molecular Trap

Piotr Skurski

Henry Eyring Center for Theoretical Chemistry, Department of Chemistry, University of Utah, Salt Lake City, Utah 84112, and Department of Chemistry, Univeristy of Gdañsk, 80-952 Gdañsk, Poland

Jack Simons*

Henry Eyring Center for Theoretical Chemistry, Department of Chemistry, University of Utah, Salt Lake City, Utah 84112

Received: September 22, 1999

The possibility of stabilizing an electronically metastable anion in a molecular trap is studied using ab initio electronic structure methods. The $^2\Pi_g$ N_2^- d-wave shape resonance state is used as a prototype for the metastable anion solute, and a pair of inwardly oriented LiCN molecules (NCLi···LiCN) is used as a prototypical trap. It is found that for the (NCLi···LiCN) trap at its local minimum geometry, the $^2\Pi_g$ state becomes electronically stable and is the ground state of the system. It is also found that, in this model trap, two other (excited) anionic states are bound ($^2\Sigma_g$ and $^2\Pi_u$) one of which is a trap-bound state and the second of which is another stabilized resonance state. Moreover, calculations performed on traps of varying strength (which we alter by varying the trap size) show that the number of bound anionic states strongly depends on the trap's strength. Detailed numerical results are presented for the (NCLi···N≡N···LiCN)$^-$ trap plus solute anion whose vertical electron detachment energy is 3.250 eV, but the results obtained are suggestive of a wide variety of such trap-stabilized anion systems.

1. Introduction

The binding of atomic and molecular cations within macromolecular cages such as crown ethers has proven very useful for separating such ions from complex solution mixtures. Analogous strategies can also be used to trap, identify, and separate electronically stable anions. However, if the lowest energy electronic state of the anion is not electronically stable (i.e., if it is a metastable resonance state), additional complications arise when devising strategies for trapping and stabilizing such species. In particular, the electrostatic potential generated by the surrounding molecular trap must serve both to lower the electronic energy of the resonance state, thus rendering it electronically stable, and to bind the resulting anion to the molecular framework of the trap itself. A potential that is strong enough to so stabilize a resonance anionic state may also be strong enough to bind the "extra" electron on its own. As a result, one is faced with the possibility that two kinds of anion states will be observed in such trap-stabilized anionic systems, states arising from resonance states of the "solute" anion and states arising as the trap's electrostatic potential binds the "extra" electron.

As a first step toward understanding the interplay between the two kinds of anion states discussed above, we have undertaken a model study in which (a) the widely studied d-wave $^2\Pi_g$ resonance state of N_2^- (which lies 2.3−2.7 eV above N_2 plus a free electron and has a width of 0.6−0.8 eV[1−10]) is used as the metastable "solute" anion and (b) we employ a structurally simple but strongly solvating "trap" consisting of two highly polar LiCN molecules with their dipoles oriented "inward" as in (NCLi···LiCN). The LiCN molecule was chosen for constructing our trap because we have significant experience in studying its electron binding energy. Specifically, we know LiCN to bind an electron (to form $NCLi^-$) by a significant amount (ca. 0.75 eV), and we thus expect two LiCN molecules oriented as above to stabilize the N_2^- resonance state by a significant amount. We realize it is unlikely that this particular (NCLi···LiCN) trap will be employed in experiments that stabilize, isolate, and remove such metastable anions. More likely candidates include, for example, the substituted macrocycles shown below which might bind an anion within their

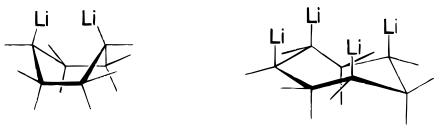

cages. However, in this our initial study of this problem, we wanted to limit the structural complexity of the trap both to control the computational difficulty and to allow us to vary the trap's solvating strength in a straightforward manner as discussed in section 3.C.

The primary goals of this (first) study of stabilization of a resonance anion state by a (strong) molecular trap were (a) to examine the nature of the resonance state as a function of the trap's stabilization strength (which we vary by varying the distance *x* between the two LiCN fragments; see Figure 1), (b) to monitor the evolution of anion states in which the electron is bound to the trap LiCN fragments (rather than to the N_2 solute) as a function of this same parameter *x*, and (c) to examine the region (*x*-values) where the solute-bound and trap-bound anion states are similar in energy and thus undergo strong mixing.

It is our belief that the results of this prototype anion plus trap study suggest the kind of behavior that is to be expected

10.1021/jp9933976 CCC: $19.00
Published on Web 01/12/2000

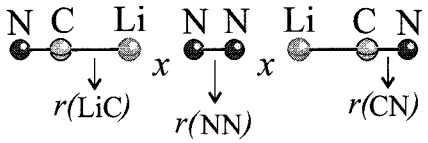

Figure 1. The MP2 equilibrium $D_{\infty h}$ geometry of the ground state of the $(NCLi\cdots N{\equiv}N\cdots LiCN)^-$ anion and the definition of geometrical parameters used in this work.

when other anions and other (experimentally more accessible) traps are considered.

2. Methods

The equilibrium geometries of the neutral and anionic species have been optimized and their harmonic vibrational frequencies calculated at the MP2 level of theory. In these calculations, the values of $\langle S^2 \rangle$ never exceeded 0.7600 for the doublet anionic states, so we are confident that spin contamination effects are not serious. The electronic stabilities of the anions in their ground states were calculated using a supermolecular approach (i.e., by subtracting the energies of the anion from those of the neutral). This approach requires the use of size-extensive methods, so we have employed Møller−Plesset perturbation theory[11] up to fourth order as well as the coupled-cluster method with single, double, and noniterative triple excitations (CCSD(T)).[12,13] In addition, the electron binding energies were analyzed within the perturbation framework described in ref 14, which generates Koopmans' Theorem (KT),[15] SCF-difference (ΔSCF), Møller−Plesset difference (MPn), and coupled cluster difference values of the binding energies. For studying the bound excited electronic states of the anions, we used the CCSD(T) method, in which cases our investigations were limited to the vertical attachment energies for those states (i.e., only single-point energy calculations were performed at the equilibrium geometry of the $D_{\infty h}$ neutral system). All calculations were performed with the *GAUSSIAN 98* (rev. A7) program,[16] on an Intel Pentium III computer and on an SGI Origin2000 numerical server. The three-dimensional plots of molecular orbitals were generated with the *Molden* program.[17]

The choice of the atomic orbital basis set used to describe the neutral molecule and the excess bound electron is very important for reproducing the correct value of the electron binding energy. The basis set must be flexible enough to describe the static charge distribution of the neutral molecular host, and to allow for polarization and dispersion stabilization of the anions upon electron attachment. For these purposes, we used the aug-cc-pVDZ basis set[18] supplemented with the diffuse functions. The addition of extra diffuse functions having very low exponents was necessary, especially in order to describe properly the bound excited states of the anions. In particular, we supplemented the aug-cc-pVDZ basis set with extra even-tempered four-term s and four-term p sets of diffuse functions centered at the midpoint of the N≡N bond. The extra diffuse s and p functions do not share exponent values. The geometric progression ratio was equal to 3.2,[19] and, for every symmetry, we started to build up the exponents from the lowest exponent of the same symmetry included in the aug-cc-pVDZ basis set designed for lithium. As a consequence, we achieved lowest exponents of 8.239746×10^{-5} and 5.521774×10^{-5} au for s and p symmetries, respectively. We choosed that particular basis set since it proved to be useful for studying the electron binding energies of the anions in which the LiCN units were used as building blocks.[20] Moreover, the preliminary estimation of the position of the $^2\Pi_g$ N_2^- resonance (by calculating the eigenvalue of the π_g virtual orbital for the neutral N_2 molecule) led to a 2.56 eV value in the chosen basis set, which is a good approximation to the values of 2.3−2.7 eV reported in the literature.[1−10]

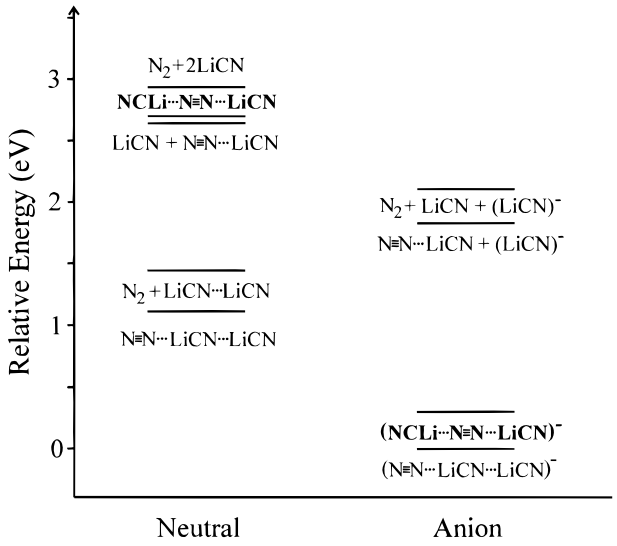

Figure 2. Schematic diagram with relative energies of the stationary points (minima) located on the potential energy surface of the neutral supermolecule ($2LiCN + N_2$) and its anionic daughter ($2LiCN + N_2 + e$).

3. Results

A. The (NCLi···LiCN) Structure as a Model "Trap". The system studied in this work consists of an N_2 "solute" molecule and two LiCN molecules that play the role of the "molecular trap" when oriented in a head-to-head manner (see Figure 1 where the relevant geometrical parameters are defined). Neither this arrangement of the neutral trap plus solute nor this arrangement of the corresponding anion is the lowest energy structure available. There exist several other structures that possess the same stoichiometry, some of which are lower in energy than the structures studied here. We examined the relative stabilities of several alternative neutral and anionic geometries in order to determine the thermodynamic stability of the $D_{\infty h}$ $(NCLi\cdots N{\equiv}N\cdots LiCN)^-$ anion considered here as a model for a molecular trap with an imbedded anion. The results pertaining to the thermodynamic stabilities of various neutral and anion isomers are summarized (at the MP2 level) in Figure 2. It is clear that the global minimum for the anion is the anion $(LiCN)_2^-$ with a weakly (van der Waals) bound N_2 molecule, and correspondingly, the global minimum for the neutral is $(LiCN)_2\cdots N_2$. This is not surprising because the linear $(LiCN)_2$ neutral possesses a very large dipole moment (21.20 D when calculated from the MP2 density) and binds an excess electron by 1.433 eV at the MP2 level. Moreover, in the $(LiCN)_2$ geometry, the repulsive dipole−dipole potential present in the (NCLi···LiCN) structure is absent.

The $D_{\infty h}$ $(NCLi\cdots N{\equiv}N\cdots LiCN)^-$ anion, which is the focus of the present work, is thermodynamically less stable than $(NCLi)_2^-\cdots N_2$ by 0.305 eV. However, because the transformation leading from $D_{\infty h}$ $(NCLi\cdots N{\equiv}N\cdots LiCN)^-$ to $(N_2\cdots NCLi\cdots NCLi)^-$ requires significant geometrical reorganization and must surmount a kinetic barrier, we conclude that the $D_{\infty h}$ $(NCLi\cdots N{\equiv}N\cdots LiCN)^-$ anion is locally stable and may be sufficiently long-lived to be experimentally accessible if it can be formed at this geometry. With this assumption in mind, and keeping in mind that (NCLi····LiCN) was chosen for study for the reasons detailed earlier, we now move on to discuss our

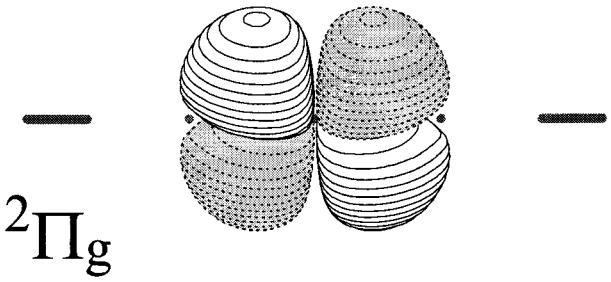

Figure 3. Singly occupied π_g molecular orbital for the $^2\Pi_g$ ground electronic state of the $(NCLi\cdots N{\equiv}N\cdots LiCN)^-$ anion.

TABLE 1: MP2 Equilibrium Geometries for the Neutral $^1\Sigma_g$ $(NCLi\cdots N{\equiv}N\cdots LiCN)$ and Ground $^2\Pi_g$ Anion Electronic State at the $D_{\infty h}$ Minima[a] (Distances in Å)

parameter	$^1\Sigma_g$ neutral	$^2\Pi_g$ anion
r(NN)	1.128	1.194
r(LiC)	1.938	2.025
r(CN)	1.198	1.199
x	2.362	1.923

[a] For the definition of the parameters r and x, see Figure 1.

examination of the two kinds of anion states discussed in the Introduction at geometries corresponding to that of the $(NCLi\cdots LiCN)$ trap.

B. The Ground $^2\Pi_g$ State of $(NCLi\cdots N{\equiv}N\cdots LiCN)^-$: The Stabilized Shape Resonance. The ground electronic state of the $D_{\infty h}$ anion at the geometry where this structure has its local minimum energy is the $^2\Pi_g$ state and consists of the d-wave shape resonance state of N_2^- that has been stabilized by the $(NCLi\cdots LiCN)$ trap. The singly occupied molecular orbital (SOMO) of this state possesses π_g symmetry and is localized on the nitrogen molecule (see Figure 3) and has the characteristic d symmetry of the π_g antibonding orbital of N_2 (which causes d-wave angular distribution of the electron ejected from the N_2^- resonance anion). The electronic stability of this anionic state strongly depends on the strength of the molecular trap, which will be discussed in detail in section 3.C.

The geometries of the $(NCLi\cdots N{\equiv}N\cdots LiCN)$ neutral and $(NCLi\cdots N{\equiv}N\cdots LiCN)^-$ anionic species were optimized at the MP2 level with constraints that preserve $D_{\infty h}$ symmetry, and the resulting optimized bond lengths are gathered in Table 1 (see also Figure 1). The neutral and anionic structures differ significantly from each other. In particular, electron attachment leads to severe (by 0.439 Å) shortening of the distances between the LiCN molecules and N_2 (described by the parameter x in Table 1 and Figure 1) and to smaller elongation of the other bonds. Since these elongations are much smaller (although not negligible) than the shortening of the x distance, the resulting total length of the negatively charged system is shorter by 0.64 Å than the neutral. This large geometry change is caused primarily by electrostatic interaction and the flexibility of this particular molecular system (i.e., the presence of the soft intermolecular degrees of freedom). It is possible to understand these geometry changes in terms of the simple electrostatic model described in Figure 4. If one considers the neutral system as two oppositely oriented local dipoles (LiCN molecules) and a quadrupole (N_2 molecule), then the repulsion between the positively charged ends of the multipoles causes elongation of the neutral species (see Figure 4, top). On the other hand, in the case of the anion, it may be considered as consisting of two repulsively oriented dipoles (LiCN) and an N_2 molecule in the center that behaves as a negatively charged monopole, since the excess electron is localized on it. As a consequence, we observe attraction between the negative monopole (N_2^-) and

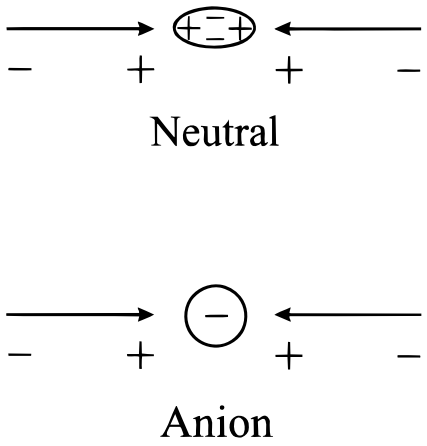

Figure 4. Schematic representation of the electrostatic interactions in the $D_{\infty h}$ $(NCLi\cdots N{\equiv}N\cdots LiCN)^-$ that lead to the shortening of its Li to N≡N distance when compared to the neutral system.

TABLE 2: Vertical Electron Binding Energies E (in eV) for the Ground $^2\Pi_g$ Electronic State of the $(NCLi\cdots N{\equiv}N\cdots LiCN)^-$ Anion at the Equilibrium $D_{\infty h}$ Geometries of the Neutral and Anionic System[a]

	$D_{\infty h}$ geometry of the neutral	$D_{\infty h}$ geometry of the anion
E^{KT}	0.779	2.438
E^{SCF}	1.723	3.750
E^{MP2}	1.478	2.962
E^{MP3}	1.793	3.510
E^{MP4}	1.562	3.067
E^{CCSD}	1.706	3.321
$E^{CCSD(T)}$	1.678	3.250

[a] All results obtained with the aug-cc-pVDZ basis set augmented with the 4s4p diffuse set centered at the midpoint of the N≡N bond.

the positive ends of the dipoles which causes the shortening of the distance x (along the soft intermolecular modes).

The vertical electron detachment and attachment energies were calculated at the $D_{\infty h}$ equilibrium geometries of the anion and the neutral system, respectively, and the results are collected in Table 2. It should be noted that the binding energies calculated for these two geometries differ significantly (by almost a factor of 2 at the CCSD(T) level) due to the large geometry relaxation of the neutral system after attaching an extra electron as described in the previous paragraph.

In the ground $^2\Pi_g$ electronic state, the anion is strongly bound even at the Koopmans' theorem level, and we observe strong orbital relaxation producing stabilizations that increase the electron binding energies by 1.312 and 0.944 eV for the geometries of the anion and the neutral, respectively. The MP series converges slowly, and even the E^{MP4} results are not conclusive. In particular, the MP2 and MP4 corrections to E are destabilizing, while the MP3 are stabilizing for both geometries. To obtain more reliable results, we also performed calculations at the coupled cluster level. The overall correlation contribution (calculated as the difference between $E^{CCSD(T)}$ and E^{SCF}; see Table 2) is destabilizing and leads to our final values of the electron binding energies of 3.250 eV (for the anionic geometry) and 1.678 eV (for the neutral geometry). It should be noted that including correlation effects is not crucial (they are responsible for the ca. 3% and 15% of the net electron binding energy for the geometry of the neutral and anion, respectively) although necessary for reproducing highly accurate values of the electron binding energies (Table 2).

C. Bound Excited States of $(NCLi\cdots N{\equiv}N\cdots LiCN)^-$: The Trap-Bound and Other Stabilized Resonance States. It is

TABLE 3: Vertical Electron Binding Energies *E* (in eV) for the Bound Excited $^2\Sigma_g$ and $^2\Pi_u$ Electronic States of the (NCLi···N≡N···LiCN)$^-$ Anion at the Equilibrium $D_{\infty h}$ Geometry of the Neutral System[a]

E	$^2\Sigma_g$ bound excited state	$^2\Pi_u$ bound excited state
E^{KT}	0.644	0.182
E^{SCF}	0.684	0.202
E^{MP2}	0.814	0.290
E^{MP3}	0.813	0.284
E^{MP4}	0.847	0.311
E^{CCSD}	0.823	0.307
$E^{CCSD(T)}$	0.842	0.318

[a] All results obtained with the aug-cc-pVDZ basis set augmented with the 4s4p diffuse set centered at the midpoint of the N≡N bond.

well-known that relatively few molecular (or atomic) anions possess bound excited states with respect to electron detachment.[21] Even in the ground state, the extra electron is usually bound too weakly to the neutral molecule to support bound excited states. There are, however, some well-known examples (e.g., tetracyanoethylene (TCNE) and 7,7,8,8-tetracyanoquinodimethane (TCNQ)[22−26]) that are able to bind an excess electron and form a few bound excited anionic states.

In the system we describe in this work, we studied the possibility of forming bound excited anionic states by calculating their energies at the CCSD(T) level for the $D_{\infty h}$ geometry of the neutral molecule, which means that vertical attachment energies were obtained. The resulting data are collected in Table 3 where the results obtained at various levels of theory are also shown. According to our findings, there are three electronically stable states of the anion at this geometry. First, is the stabilized shape resonance ground anionic state $^2\Pi_g$ that we have already analyzed in section 3.B. The next two states ($^2\Sigma_g$ and $^2\Pi_u$) have vertical electron binding energies estimated at the KT level of 0.64 and 0.18 eV, respectively. For these states, orbital relaxation effects are relatively unimportant, in contrast to the $^2\Pi_g$ state. However, correlation contributions are more important for reproducing correct values of the electron binding energies for the $^2\Sigma_g$ and $^2\Pi_u$ states than for $^2\Pi_g$ state; they are responsible, respectively, for ca. 19% and 36% of the net electron binding energy (see Table 3). Our final values of the vertical attachment energies are 0.842 eV for the $^2\Sigma_g$ state and 0.318 eV for the $^2\Pi_u$.

The physical origins of the $^2\Sigma_g$ and $^2\Pi_u$ states may be understood by monitoring the evolution of their binding energies and orbital character as the distance *x*, and thus the stabilizing strength of the trap, is varied. Retaining $D_{\infty h}$ symmetry, we varied the *x* parameter (see Figure 1) between 1.923 Å (which corresponds to x_{eq}) and 50 Å in a series of single-point calculations. At every point, we calculated the energies of all electronically stable anionic states as well as the energy of the neutral. The results are depicted in Figure 5 (for which we limited the range for *x* to 17 Å because the data for $x = 17-50$ Å did not provide any qualitatively new information). The corresponding singly occupied molecular orbitals in the anionic systems are depicted in Figure 6 for three selected ranges of *x*: part A (for $x > 6$ Å), part B (for $x = 4-6$ Å), part C (for $x = 1.923-4$ Å), and part D (for $x = x_{eq}=1.923$ Å).

In region A, the trap plus solute system consists essentially of two separated LiCN molecules, each of which can bind an extra electron to form a dipole-bound state, with an N_2 molecule in the middle. Not surprisingly, at such geometries we find two anionic states $^2\Sigma_g$ and $^2\Sigma_u$, (see Figure 6A and Figure 5) whose energies are nearly degenerate and whose single occupied orbital

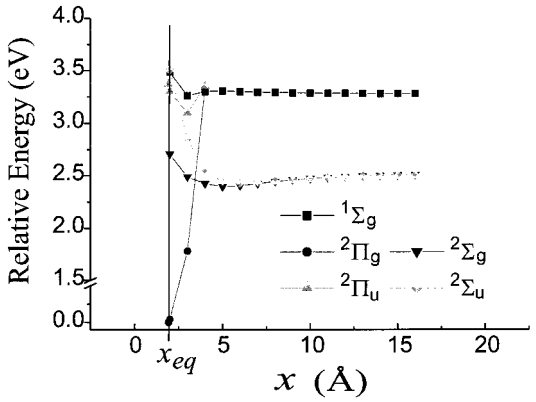

Figure 5. Relative energies of various anionic states of (NCLi···N≡N···LiCN) at the stretched and equilibrium $D_{\infty h}$ geometries compared to the energy of the neutral system (squares). The *x* parameter measures the distance between a Li atom and the nearest nitrogen atom in the N_2 molecule and is identical for both sides of the system in order to preserve the $D_{\infty h}$ symmetry of the anion (see also Figure 1). The value x_{eq} corresponds to $x = 1.923$ Å, which is the equilibrium distance for the optimized geometry of the ground $^2\Pi_g$ state of the anion.

lobes are localized on the LiCN units and not distorted by the presence of the N_2 molecule. At these geometries, the N_2 molecule can bind the excess electron to form the shape resonance state; however, this state is not bound with respect to the neutral system, and its energy (∼2.3 eV above the neutral) is not shown in Figure 5. It should be noted that the doubly charged anionic system is also stable relative to the singly charged anion in this region because each of the LiCN units can bind one extra electron when they are separated by distances large enough to overcome their mutual Coulomb $1/r$ repulsion. The stability of the dianion vanishes when *x* approaches 9 Å.

In region B, the two LiCN molecules are close enough to N_2 and to each other to interact. As a consequence, the orbital lobes localized on the LiCN units are perturbed by the exclusion and orthogonality interactions with the N_2. Again, in this region, we find two stable anionic states ($^2\Sigma_g$ and $^2\Sigma_u$) (see Figure 6B and Figure 5), but their energies are now split due to their differential interactions with the N_2 (the g state becomes more stable than the u). The $^2\Pi_g$ N_2^- resonance state drops in energy as *x* decreases (from 0.20 eV above the neutral for $x = 6$ Å, to 0.12 eV for $x = 4$ Å, when estimated via Koopmans' theorem); however, this state is still not shown in Figure 5 in region B because it is not yet stable relative to the neutral molecule.

In region C, we find even more electronically stable excited states as two $^2\Pi$ states also become stable. One is the $^2\Pi_g$ shape resonance state whose energy decreases very rapidly as *x* approaches x_{eq}; the energy curve for this state intersects the other curves in the 3−4 Å region, and the $^2\Pi_g$ state subsequently becomes the ground state of the anion. The second stable $^2\Pi$ state is the $^2\Pi_u$ state whose energy curve possesses a shallow minimum at $x \approx 4$ Å. This state can be considered as another stabilized resonance state of N_2^-, although its singly occupied orbital also has significant contributions from AOs centered on the Li atoms. In region C, the $^2\Sigma_g$ and $^2\Sigma_u$ states are still stable, but their energies increase as *x* approaches its equilibrium value. Moreover, their orbital natures change significantly because the perturbations that they are exposed to are very severe in this region (see Figure 6C).

Region D denotes the equilibrium geometry of the $^2\Pi_g$ anion (i.e., $x = x_{eq}= 1.923$ Å). The $^2\Sigma_u$ state, although plotted in Figure 6D, is no longer stable with respect to the neutral system (see also Figure 5) and its SOMO has evolved into a pair of "donuts" because of exclusion forces due to the N_2 molecule. The orbitals

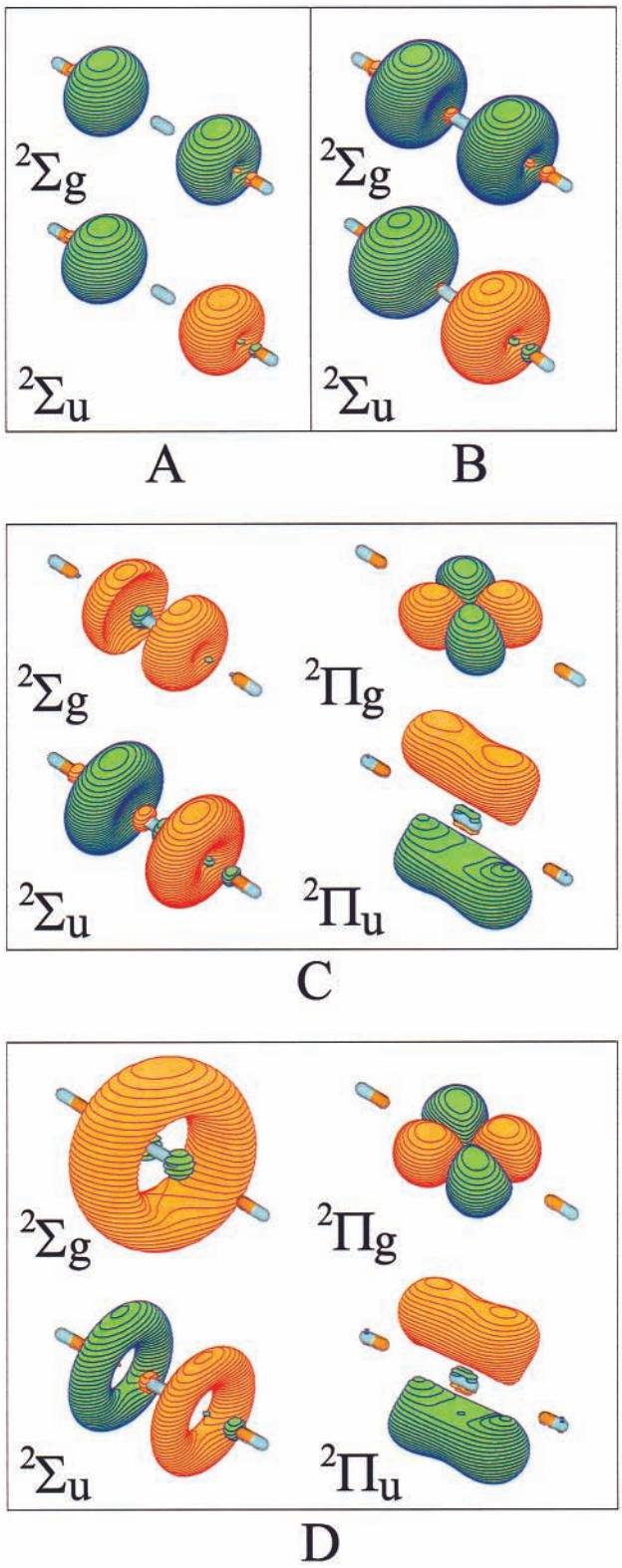

Figure 6. The singly occupied molecular orbitals for various anionic states of (NCLi···N≡N···LiCN) at the stretched $D_{\infty h}$ (A, B, and C) structures and at the equilibrium $D_{\infty h}$ geometry (D) of the ground $^2\Pi_g$ state of the anion. The orbitals correspond to $x = 7$ Å (A), $x = 5$ Å (B), $x = 3$ Å (C), and $x = 1.923$ Å (D) (see Figure 1 for the definition of the x parameter).

of the $^2\Pi_g$ and $^2\Pi_u$ states are nearly unchanged relative to what is seen in region C, but the g state is lower in energy than any other state and the u state is slightly below the neutral and thus remains stable. The $^2\Sigma_g$ state is also stable, but its orbital nature

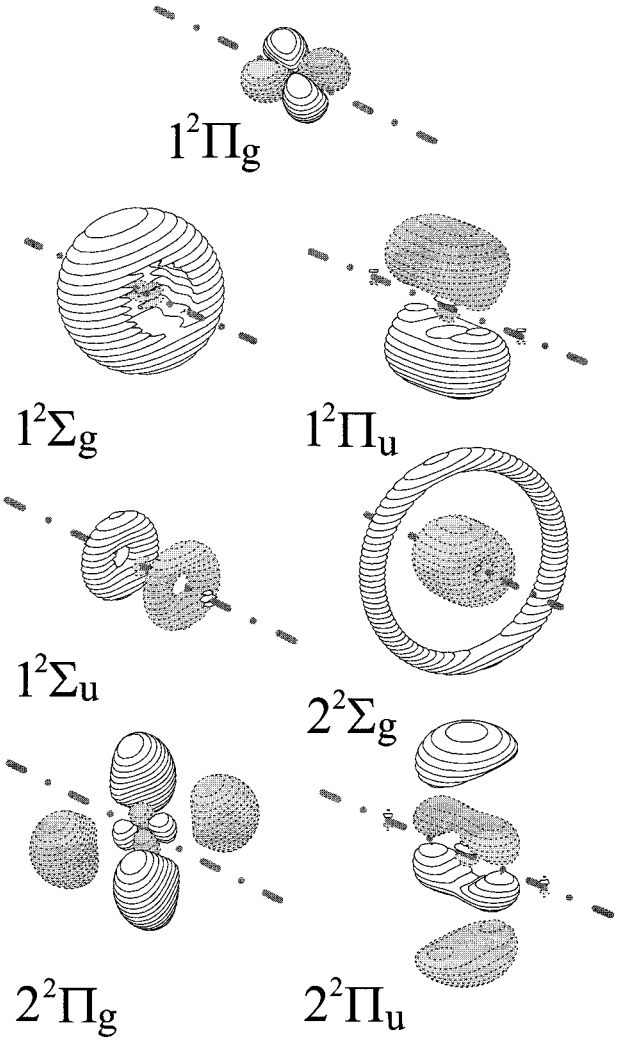

Figure 7. Singly occupied molecular orbitals for various anionic states of $((NCLi)_2\cdots N\equiv N\cdots(LiCN)_2)$ at the equilibrium (MP2 level) $D_{\infty h}$ geometry of the ground $^2\Pi_g$ state of the anion.

is significantly changed and consists of two lobes localized on the N_2 molecule and primarily a large donut surrounding the molecular axis.

D. An Even Stronger Molecular Trap. To stabilize a larger number of excited states, an even stronger prototype molecular trap was designed by adding yet another LiCN to each side of the previous trap. Since this system possesses 14 heavy atoms, we limited our calculations to the Koopmans', SCF, and MP2 levels. The calculated vertical detachment energies of the stabilized resonance state (at the anion geometry optimized at the MP2 level) are 2.078 eV (KT), 3.033 eV (SCF), and 2.731 eV (MP2). This $1^2\Pi_g$ state is the ground state of the anion, but now there are six bound excited anionic states ($1^2\Sigma_g$, $1^2\Pi_u$, $1^2\Sigma_u$, $2^2\Pi_g$, $2^2\Sigma_g$, and $2^2\Pi_u$), the first three of which are analogous to those seen for the $(NCLi\cdots N\equiv N\cdots LiCN)^-$ case. The vertical electronic stabilities calculated for this geometry at the MP2 level for the six bound excited states are 1.782, 1.237, 1.133, 0.270, 0.153, and 0.101 eV, respectively. The singly occupied molecular orbitals for the ground $^2\Pi_g$ state and for the bound excited anionic states are depicted in Figure 7. The SOMOs that correspond to the lower lying states (i.e., $1^2\Pi_g$, $1^2\Sigma_g$, $1^2\Pi_u$, and $1^2\Sigma_u$) are similar to those shown previously for $(NCLi\cdots N\equiv N\cdots LiCN)^-$ (Figure 6D). The SOMOs for less stable states possess more complicated structures; in particular, they have one more nodal plane than their more stable counterparts. These results and those of section 3.C clearly show

that traps sufficiently strong to render metastable (by ~2 eV) anion states bound are also strong enough to form other anion states that may compete with the stabilized solute state.

4. Conclusions

Our results indicate that it is possible to stabilize metastable anion states such as the $^2\Pi_g$ d-wave shape resonance state of N_2^- in molecular traps as strongly stabilizing as that consisting of two LiCN molecules with their dipoles directed inward. In such a trap, the former resonance state becomes electronically stable and is the ground state of the anion at some geometries. In the $(NCLi\cdots N\equiv N\cdots LiCN)^-$ case examined here, the vertical detachment energy of this state of the anion was found to be 3.250 eV. The electronic stability of this state strongly depends on the size (and the solvating strength) of the trap, and this state becomes unbound as the distance x (see Figure 5), through which the trap's solvating strength is altered, approaches 4 Å.

Two excited anionic states of this system are also electronically bound. One has $^2\Sigma_g$ symmetry and consists of a trap-bound state, and the other has $^2\Pi_u$ symmetry. These two states are bound by 0.842 and 0.318 eV, respectively. The number of bound excited states may be increased by changing the "strength" of the trap (e.g., six bound excited states were found for the $((NCLi)_2\cdots N\equiv N\cdots(LiCN)_2)^-$ species and the number of bound states varies in $(NCLi\cdots N\equiv N\cdots LiCN)^-$ as x varies).

These results suggest that (a) metastable anion states can be stabilized by molecular traps of sufficient "strength" and of appropriate size to bind the resulting stable solute anion, (b) sufficiently strongly solvating traps can bind the "extra" electron by themselves, as a result of which, (c) both trap-stabilized resonance states and trap-bound anion states can arise.

We believe that the existence of the above two classes of bound anion states should be subjected to experimental (probably gas-phase spectroscopic) study.

Acknowledgment. This work was supported by the NSF Grant CHE9618904 to J.S. and the Polish State Committee for Scientific Research (KBN) Grant DS/8000-4-0026-9. The computer time provided by the Center for High Performance Computing at the University of Utah is also gratefully acknowledged. The authors thank Dr. M. Gutowski for his valuable comments.

References and Notes

(1) Herzenberg, A.; Mandl, F. *Proc. R. Soc.* **1962**, *A270*, 48.
(2) Schulz, G.; Koons, H. C. *J. Chem. Phys.* **1966**, *44*, 1297.
(3) Herzenberg, A. *J. Phys.* **1968**, *B1*, 548.
(4) Birtwistle, D. T.; Herzenberg, A. *J. Phys.* **1971**, *B4*, 53.
(5) Schulz, G. *Rev. Mod. Phys.* **1973**, *45*, 423.
(6) Schneider, B. L.; Le Courneuf, M.; Lau, V. K. *Phys. Rev. Lett.* **1979**, *43*, 1927.
(7) Rescigno, T. N.; Orel, A. E.; McCurdy, C. W. *J. Chem. Phys.* **1980**, *73*, 6347.
(8) Hazi, A. U.; Rescigno, T. N.; Kurrila, M. *Phys. Rev. A* **1981**, *A23*, 1089.
(9) Donnelly, R. A. *Int. J. Quantum Chem.* **1982**, *S16*, 653.
(10) Gianturco, F. A.; Schneider, F. *J. Phys. B* **1996**, *29*, 1175.
(11) Møller, C.; Plesset, M. S. *Phys. Rev.* **1934**, *46*, 618.
(12) Bartlett, R. J.; Stanton, J. F. In *Reviews in Computational Chemistry*; Lipkowitz, K. B., Boyd, D. B., Eds.; VCH Publishers: New York, 1994; Vol. V.
(13) Taylor, P. R. In *Lecture Notes in Quantum Chemistry II*; Roos, B. O., Ed.; Springer-Verlag: Berlin, 1994.
(14) Gutowski, M.; Skurski, P. *J. Phys. Chem. B* **1997**, *101*, 9143.
(15) Koopmans, T. *Physica* **1934**, *1*, 104.
(16) Frisch, M. J.; Trucks, G. W.; Schlegel, H. B.; Scuseria, G. E.; Robb, M. A.; Cheeseman, J. R.; Zakrzewski, V. G.; Montgomery, J. A., Jr.; Stratmann, R. E.; Burant, J. C.; Dapprich, S.; Millam, J. M.; Daniels, A. D.; Kudin, K. N.; Strain, M. C.; Farkas, O.; Tomasi, J.; Barone, V.; Cossi, M.; Cammi, R.; Mennucci, B.; Pomelli, C.; Adamo, C.; Clifford, S.; Ochterski, J.; Petersson, G. A.; Ayala, P. Y.; Cui, Q.; Morokuma, K.; Malick, D. K.; Rabuck, A. D.; Raghavachari, K.; Foresman, J. B.; Cioslowski, J.; Ortiz, J. V.; Stefanov, B. B.; Liu, G.; Liashenko, A.; Piskorz, P.; Komaromi, I.; Gomperts, R.; Martin, R. L.; Fox, D. J.; Keith, T.; Al-Laham, M. A.; Peng, C. Y.; Nanayakkara, A.; Gonzalez, C.; Challacombe, M.; Gill, P. M. W.; Johnson, B.; Chen, W.; Wong, M. W.; Andres, J. L.; Gonzalez, C.; Head-Gordon, M.; Replogle, E. S.; Pople, J. A. *Gaussian 98*, revision A.7; Gaussian, Inc.: Pittsburgh, PA, 1998.
(17) Schaftenaar, G. *MOLDEN*; CAOS/CAMM Center: The Netherlands, 1991.
(18) Kendall, R. A.; Dunning, T. H., Jr.; Harrison, R. J. *J. Chem. Phys.* **1992**, *96*, 6796. Woon, D. E.; Dunning, T. H., Jr. *J. Chem. Phys.* **1993**, *98*, 1358.
(19) Gutowski, M.; Simons, J. *J. Chem. Phys.* **1990**, *93*, 3874.
(20) Skurski, P.; Gutowski, M.; Simons, J. *J. Chem. Phys.* **1999**, *111*, 9469.
(21) Simons, J.; Jordan, K. D. *Chem. Rev.* **1987**, *87*, 535.
(22) Klots, C. E.; Compton, R. N.; Raaen, V. F. *J. Chem. Phys.* **1974**, *60*, 1177.
(23) Compton, R. N.; Cooper, C. D. *J. Chem. Phys.* **1977**, *66*, 4325.
(24) Brinkman, E. A.; Günter, E.; Brauman, J. I. *J. Chem. Phys.* **1991**, *91*, 6185.
(25) Brinkman, E. A.; Günter, E.; Schaefer, O.; Brauman, J. I. *J. Chem. Phys.* **1994**, *100*, 1840.
(26) Zakrzewski, V. G.; Dolgounitcheva, O.; Ortiz, J. V. *J. Chem. Phys.* **1996**, *105*, 5872.